Paleontological Journal, Vol. 37, No. 6, 2003, pp. 653–664. Translated from Paleontologicheskii Zhurnal, No. 6, 2003, pp. 94–104.

A New Genus of the Erinaceidae (Insectivora, Mammalia) from the Oligocene of Mongolia

A. V. Lopatin

Paleontological Institute, Russian Academy of Sciences, Profsoyuznaya ul. 123, Moscow, 119997 Russia
e-mail: alopat@paleo.ru

Received October 1, 2002

Abstract—On the basis of an almost complete skull with the lower jaw from the Oligocene Shand-Gol Formation of the Ulan-Khureh locality in Mongolia, a new erinaceid genus and species, *Scymnerix tartareus*, is described. This is a small hedgehog whose skull is approximately 3 cm long. *Scymnerix* shows convergent similarity to short-faced hedgehogs (Brachyericinae) in certain cranial and dental traits, such as the shortened facial region of the skull, high and raised posterior part of the zygomatic arch, single-rooted I^3, the absence of M^3, the structure of P^4–M^2, strongly enlarged I_2, and the presence of enamel sculpture on the labial surface of teeth. However, the basicranium structure of *Scymnerix* suggests that it should be referred to true hedgehogs (Erinaceinae). Structural cranial and dental features of *Scymnerix* clearly distinguish it from both Amphechinini and Erinaceini and enable one to rank this genus as a separate tribe, Scymnericini tr. nov.

Key words: Hedgehogs, Erinaceidae, new taxa, Oligocene, Mongolia.

INTRODUCTION

To date, nine erinaceid species have been discovered in the Early Oligocene Shandgolian Fauna of Central Asia (Matthew and Granger, 1924; Trofimov, 1960; McKenna and Holton, 1967; Mellett, 1968; Sulimski, 1970; Huang, 1984; Storch and Dashzeveg, 1997; Lopatin, 2002; Lopatin and Zazhigin, 2003). They include two species of the subfamily Tupaiodontinae, i.e., *Tupaiodon morrisi* Matthew et Granger, 1924 and *Zaraalestes minutus* (Matthew et Granger, 1924) [= *Ictopidium tatalgolensis* Sulimski, 1970], and two species of the subfamily Brachyericinae, *Exallerix hsandagolensis* McKenna et Holton, 1967 and *E. manahan* Lopatin et Zazhigin, 2003. True hedgehogs (Erinaceinae) are represented by five members of the tribe Amphechinini: *Palaeoscaptor acridens* Matthew et Granger, 1924, *Amphechinus rectus* (Matthew et Granger, 1924), *A.* cf. *minimus* Bohlin, 1942, *A.* cf. *kansuensis* Bohlin, 1942, and *A. gigas* Lopatin, 2002. These species are mainly represented by lower jaw fragments.

In the present paper, a new genus and species of the subfamily Erinaceinae from the Oligocene of Mongolia is described. The material consists of an almost complete skull with the lower jaw, which was in natural articulation before the preparation of the specimen. It comes from the Shand-Gol Formation of the Ulan-Khureh locality (collected by the Joint Soviet–Mongolian Paleontological Expedition headed by V.Yu. Reshetov in 1979). The specimen is housed at the Paleontological Institute of the Russian Academy of Sciences, Moscow (PIN).

The terminology and measurements of the skull, lower jaw, and teeth follow Butler (1948, 1956, 1980), McDowell (1958), Rich (1981), and Frost *et al.* (1991); the terminology of elements of the tympanic region of the skull follows Klaauw (1931), Novacek (1986), and MacPhee *et al.* (1988).

SYSTEMATIC PALEONTOLOGY

Family Erinaceidae Fischer, 1817

Subfamily Erinaceinae Fischer, 1817

Tribe Scymnericini Lopatin, tr. nov.

Type genus. *Scymnerix* Lopatin, gen. nov.

Diagnosis. Facial region of skull short, approximately 30% of total skull length; infraorbital foramen located above P^3, anterior orbital border located above P^4, and anterior end of zygomatic arch located above M^1. Antorbital fossa present. Lacrimal foramen on antorbital crest. Posterior region of zygomatic arch relatively high and raised. Palatine fissures small. Nasopharyngeal fossa undeveloped. Interparietal very large. Paroccipital processes small. Anterior edge of occipital condyles not emarginated. Postglenoid foramen isolated from glenoid fossa by entoglenoid process. Ectotympanic small and shaped into incomplete ring open caudally. Mandibular condyle located on level with tooth row. Dental formula $I^3/_2C^1/_1P^3/_2M^2/_3$. I^3 and P^2 single-rooted. C^1 small. Lingual lobe of P^4 short. M^2 reduced and lacking hypocone. I_2 strongly enlarged. P_4 provided with rudimentary metaconid and high paraconid. Trigonid of M_1 high and relatively narrow. M_2

reduced. M_3 rudimentary, single-rooted, and column-like. Labial surface of teeth with enamel sculpture shaped into longitudinal rows of tubercles.

Generic composition. Type genus.

Comparison. The new tribe differs from Erinaceini Fischer, 1817 and Amphechinini Gureev, 1979 in the short facial region of the skull; the structure of the zygomatic arch; weak paroccipital processes; single-rooted I^3; reduced M^2; the shape and structure of P_4, M_1, and M_2; and the presence of the enamel sculpture on the teeth. In addition, it differs from Erinaceini in the small palatine fissures, the position of the postglenoid foramen, the absence of a nasopharyngeal fossa, the large interparietal, the structure of the ectotympanic, the low position of the mandibular condyle, the shape of P^4, the absence of M^3, strongly enlarged I_2, and rudimentary M_3. Additional distinctions from Amphechinini are the position of the lacrimal foramen, which is located in the antorbital crest (rather than in the orbit); nonemarginated anterior edge of the occipital condyle; the small upper canine; and the single-rooted P^2.

Genus *Scymnerix* Lopatin, gen. nov.

Etymology. From the Latin *scymnus* (juvenile animal, cub) and the Latin *erix* (hedgehog).

Type species. *S. tartareus* sp. nov.

Diagnosis. The same as the diagnosis of the tribe.

Species composition. Type species.

Scymnerix tartareus Lopatin, sp. nov.

Plate 3, figs. 1–7

Etymology. From the Latin *tartareus* (Tartarean, underground).

Holotype. PIN, no. 3106/80, skull with the lower jaw; Mongolia, Ulan-Khureh locality; Lower Oligocene, Shand-Gol Formation.

Description (Figs. 1–5). A small-sized hedgehog, the skull is approximately 30 mm long; the zygomatic arches are approximately 20 mm wide (Pl. 3, fig. 1). The skull is wedge-shaped and relatively wide and short. The cranial base is wide, the zygomatic arches are widely spaced, and the facial region is short. Posteriorly, the skull gradually increases in depth and reaches the maximum at the glenoid fossae.

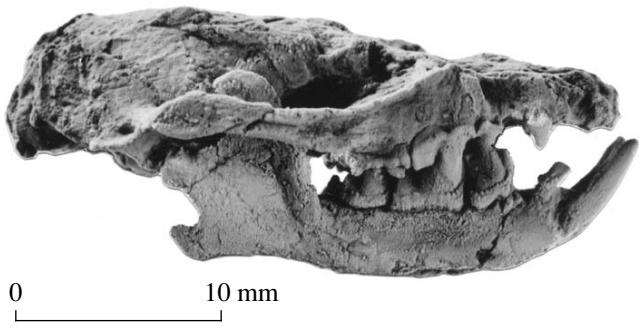

Fig. 1. *Scymnerix tartareus* sp. nov., holotype PIN, no. 3106/80, skull in articulation with the lower jaw.

The skull is slightly distorted, i.e., weakly dorsoventrally flattened. Anterior to the right canine and the alveolus of left I^2, the rostrum is broken off. A large part of the left zygomatic arch is lost (reconstructed on the basis of the right side). The surfaces of some cranial bones (in particular, in the facial region and the palate) are damaged.

Facial region (Figs. 1, 2a, 3a). The rostrum is short and narrow. The nasals are very narrow, extend posteriorly to the level of the anterior orbital rim, and adjoin the frontals. Because of strong fragmentation, the extent to which the dorsal portions of the premaxillae stretch out posteriorly and whether or not they reach the frontals are open questions; however, they most likely reached the frontals in line with the infraorbital foramina. The posterior boundary of the dorsal process of the maxilla is slightly anterior to the level of the nasofrontal suture. The suture between the premaxilla and maxilla is well-pronounced on the ventral and lateral sides of the rostrum, its ventral portion extends between the alveoli of the posterior incisor and the canine. The infraorbital foramen is small, round, and located above the center of P^3. The anterior orbital rim is located above the anterior region of P^4. The antorbital crest is stout. No traces of an isolated lacrimal are observed. The lacrimal foramen is small and located anterior to the orbit in the depression on the antorbital crest.

The zygomatic arches are narrow, relatively high, and gently curve laterally; posteriorly, they are slightly raised. The base of the zygomatic arch is level with M^1. The anterior end of the zygomatic arch is formed by a long zygomatic process of the maxilla. Its dorsal edge is very narrow and ridgelike. The anterolateral side of the arch has a small antorbital (nasolabialis) fossa, which posteriorly becomes a relatively deep longitudinal groove and provides the attachment area for the rostral musculature. The groove extends to the middle of the zygomatic arch where the zygomatic processes of the maxilla and squamosal adjoin the jugal. The jugal is very small and occupies a ventral position; in lateral view, its projection wedges in between two other bones (Fig. 3a). The lateral portion of the zygomatic process of the squamosal is shaped into a vertically expanded plate, as is observed in *Brachyerix macrotis* Matthew, 1913 (Rich and Rich, 1971, fig. 1), whose surface is slightly concave.

Palate (Fig. 2b). Most of the palate is formed by the maxilla. The ventral portion of the suture between the premaxilla and maxilla extends anteriorly to the level of the posterior part of the alveolus of I^2 where it turns medially. Because of poor preservation, it is difficult to recognize the size and shape of the palatine fissures and the position of the boundary between the maxilla and palatine. However, the central part of the bony palate, which is damaged between the molar rows, probably

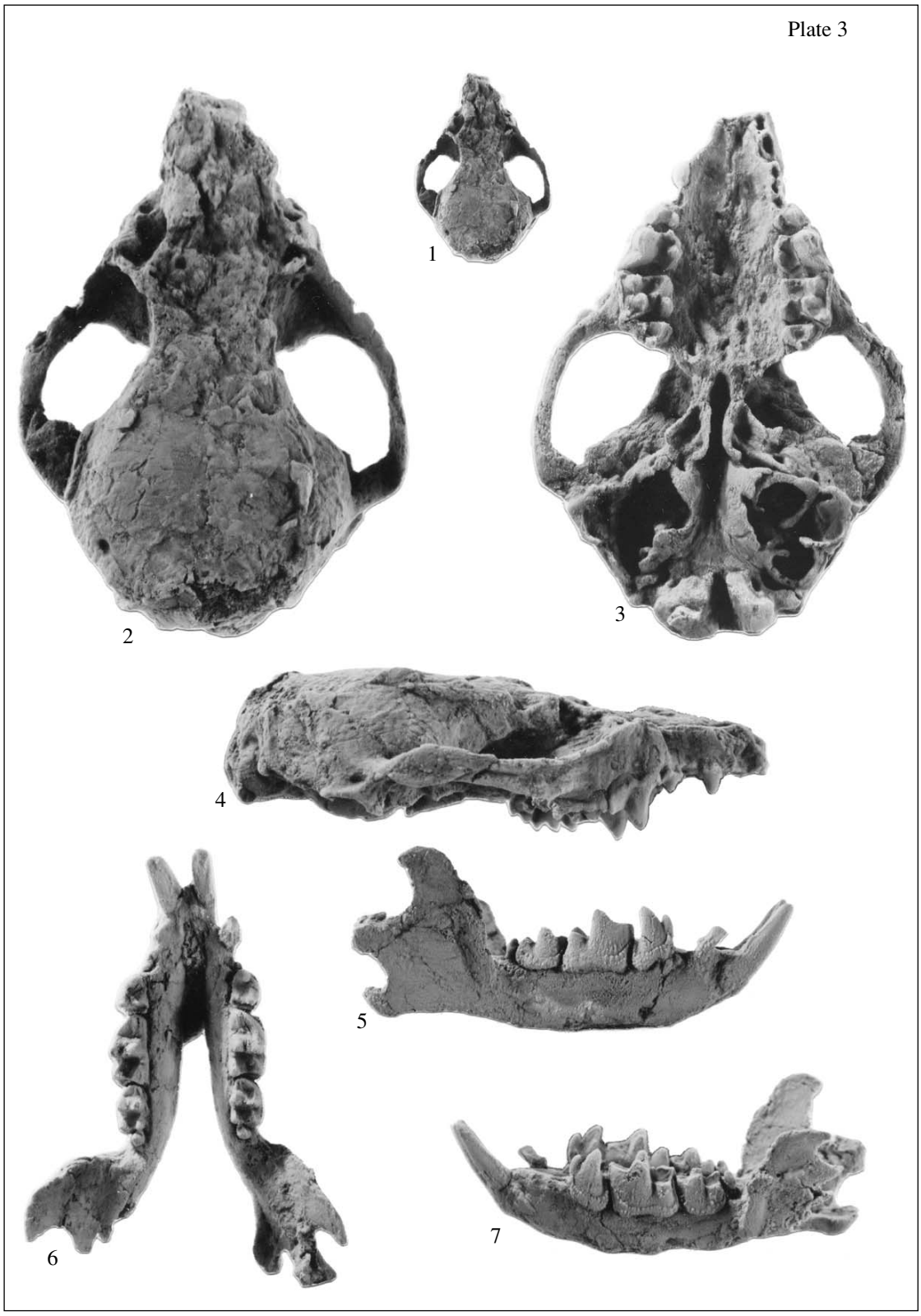

Explanation of Plate 3

Figs. 1–7. *Scymnerix tartareus* sp. nov., holotype PIN, no. 3106/80, skull with the lower jaw: (1) general appearance, dorsal view, ×1; (2) skull, dorsal view, ×3; (3) skull, ventral view, ×3; (4) skull, right lateral view, ×3; (5) lower jaw, right lateral view, ×3; (6) lower jaw, occlusal surface, ×3; and (7) lower jaw, left lateral view, ×3.

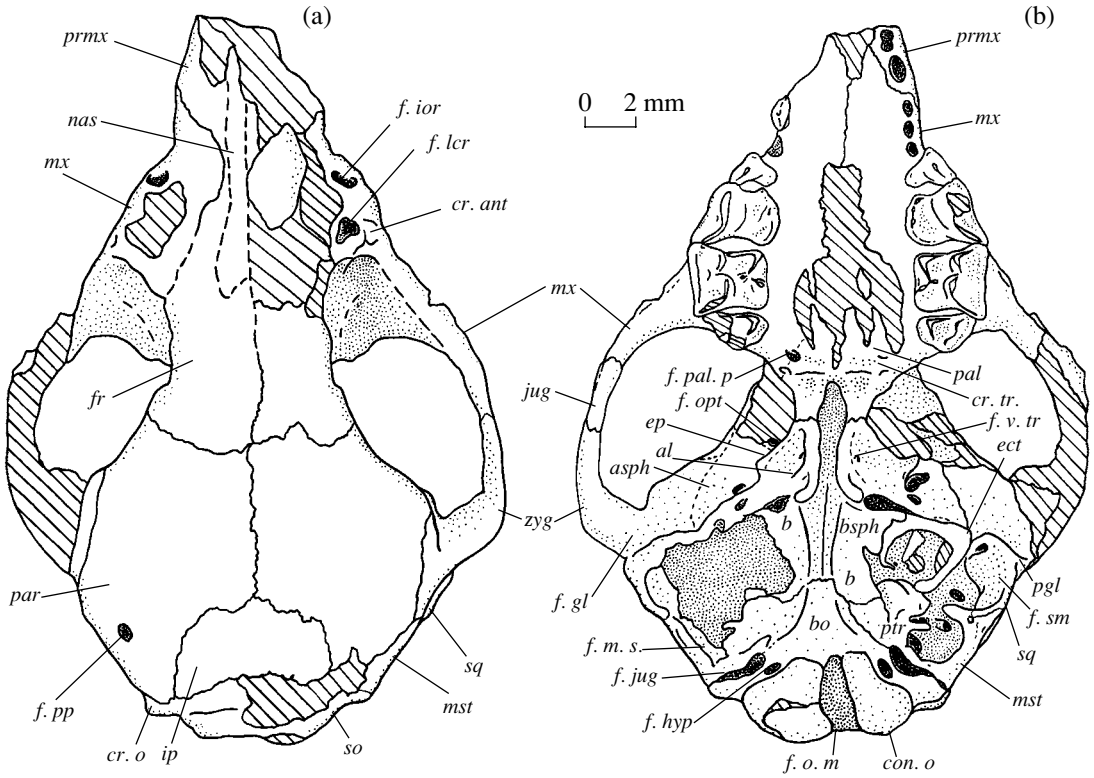

Fig. 2. *Scymnerix tartareus* sp. nov., holotype PIN, no. 3106/80, skull: (a) dorsal and (b) ventral views. Designations: (*al*) internal pterygoid (alisphenoid) process, (*asph*) alisphenoid, (*b*) tympanic bulla, (*bo*) basioccipital, (*bsph*) basisphenoid, (*con. o*) occipital condyle, (*cr. ant*) antorbital crest, (*cr. o*) occipital crest, (*cr. tr*) transverse crest (postpalatine torus), (*ect*) ectotympanic, (*ep*) external pterygoid (epipterygoid) process, (*f. gl*) glenoid fossa, (*f. hyp*) hypoglossal (condylar) foramen, (*f. ior*) infraorbital foramen, (*f. jug*) jugular (posterior lacerate) foramen, (*f. lcr*) lacrimal foramen, (*f. m. s*) fossa for the stapedius muscle, (*f. o. m*) foramen magnum, (*f. opt*) optic foramen, (*f. pal. p*) posterior palatine foramen, (*f. pp*) postparietal foramen, (*f. sm*) suprameatal fossa, (*f. v. tr*) transverse venous foramen, (*fr*) frontal, (*f. t. E*) foramen of the Eustachian tube, (*ip*) interparietal, (*jug*) jugal, (*mst*) mastoid process of the petrosal (mastoid), (*mx*) maxilla, (*nas*) nasal, (*pal*) palatine, (*par*) parietal, (*pgl*) postglenoid process, (*prmx*) premaxilla, (*ptr*) petrosal, (*sq*) squamosal, (*so*) supraoccipital, and (*zyg*) zygomatic process of the squamosal.

corresponds in its position to the palatine. Thus, the palatine–maxillary suture could extend anteriorly to the anterior part of M^1 or the posterior part of P^4. The palatine fissures are most likely relatively small; however, they are elongated, being similar to those of other Erinaceinae. Posteriorly, the palate is limited by a relatively stout transverse crest (postpalatine torus), which is located far posterior to M^2. The posterior palatine foramina are relatively large and pierce the lateral segments of the postpalatine torus. The palatines only slightly project beyond the transverse crest and terminate anterior to the pterygoid processes. The postpalatine torus spine is undeveloped.

Orbitotemporal region (Fig. 3a). The anteromedial wall and the orbital floor are formed by the maxilla. The frontal and parietal form the dorsal area of the medial wall. The boundaries between other bones of the orbital wall are indiscernible because of poor preservation. Three foramina are clearly pronounced on the right side. The anteriormost foramen, for. orbitonasale, is located in the palatine on level with the anterior edge of the posterior nasal passage. Posterior to this passage (far caudal to the postpalatine torus), there is a large foramen, which probably unites the sphenopalatine and suboptic foramina. The optic foramen is relatively small and located more dorsally. The foramen ovale is moderately large and located directly lateral to the end of the external pterygoid process anterior to the tympanic bulla.

Skull roof and occiput (Figs. 2a, 3a). The skull roof is weakly convex in lateral view. The sagittal and frontal crests are undeveloped. The frontals are short, substantially shorter than the parietals. The postorbital processes are weak. The frontals come into contact with the parietals posterior to the interorbital constriction in line with the middle of the zygomatic arches. The parietals are large, convex, form most of the skull roof and the dorsal region of the lateral braincase walls, and overlap the squamosals. Relatively large postparietal foramina (one on each side of the skull) are located in line with the anterior region of the interparietal slightly dorsal to the sutures between the parietal and squamosal. The interparietal is very large and semicircular in shape. Just posterior to the zygomatic process, the

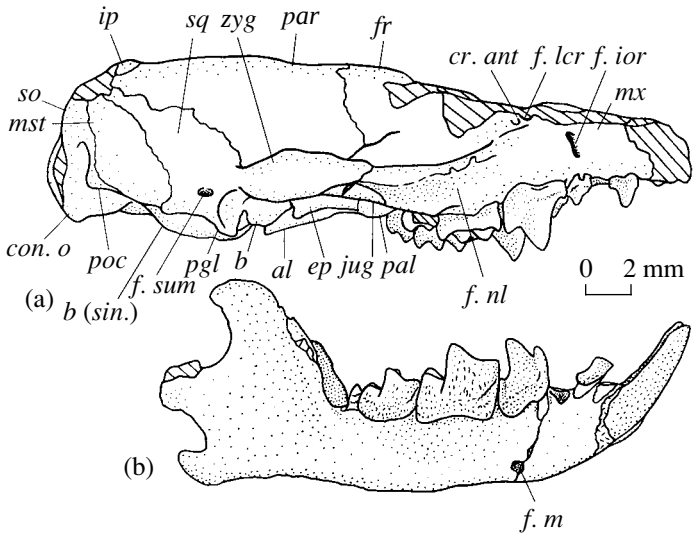

Fig. 3. *Scymnerix tartareus* sp. nov., holotype PIN, no. 3106/80, skull with the lower jaw, right lateral view: (a) skull and (b) lower jaw. Designations: (*f. m*) mental foramen, (*f. nl*) antorbital (nasolabialis) fossa, (*f. sum*) suprameatal foramen, (*poc*) paroccipital process, and (*sin*) left; for other designations, see Fig. 2.

squamosal contains a small foramen located somewhat dorsal to the crest of the postglenoid process, which separates the glenoid fossa from the suprameatal fossa. This is the suprameatal foramen (or for. subsquamosum sensu Butler, 1956), which provides passage for the vein from the upper sinus of the petrosal to the external jugular vein. Another small foramen in the squamosal is located near its contact with the mastoid process of the petrosal (mastoid) dorsal to the tympanohyal. This is the opening of a canal that enters the intracranial sinus of the squamosal. Near the boundary with the parietal, the mastoid contains two small foramina open in the sinus of the petrosal.

The occiput is narrow; in lateral view, it is convex and round. The occipital crests are weak, positioned far from the squamosal–mastoid sutures, and extend lateral to the sutures between the mastoids and exoccipitals. The supraoccipital is positioned subvertically and is comparable in area to the interparietal. The paroccipital processes are small. The foramen magnum is circular in shape.

Cranial base (Figs. 2b, 4). The internal pterygoid (alisphenoid) processes are narrow and curve laterally like a hook. The hook (hamulus) of the internal pterygoid process is clearly differentiated from the base, i.e., the posterior edge of the base is located near the foramen ovale, and the hook reaches the line of the anteromedial corner of the tympanic bulla and the foramen of the Eustachian tube. The base of the lateral wall of the internal pterygoid process contains a small transverse venous foramen. The external pterygoid (epipterygoid) process is shaped into a laterally curving lamina with a pointed triangular apex. Somewhat lateral to its posterior end, the anterior wall of the auditory capsule contains a large foramen for the ramus inferior of the stapedius artery. Laterally, the tympanic process of the alisphenoid closely approaches the line of the postglenoid foramen. The basisphenoid is not perforated, the nasopharyngeal fossa (= basisphenoid pit = nasopharyngeal pocket sensu Butler, 1948) is absent.

The suture between the basioccipital and basisphenoid is located in line with the middle of the auditory capsule. The suture between the basioccipital and the rostral tympanic process of the petrosal is well-pronounced. The longitudinal keel of the basioccipital is indiscernible.

The occipital condyles are large. The hypoglossal (condylar) foramen (for. hypoglossus s. condylaris) is positioned close to the condyle; however, the anterior edge of the condyle is nonemarginated. Just anterolateral to the hypoglossal foramen, the suture between the basioccipital and the mastoid contains a large fissure-like jugular (posterior lacerate) foramen.

The glenoid fossa is extensive and deeply concave in the posterior region. The postglenoid process is high and short. The postglenoid foramen looks like an exit from a narrow vertical groove, which is partially open medially. It is small, fissure-like, separated from the glenoid fossa by the entoglenoid process, and located in the medial part of the posterior wall of the postglenoid process just lateral to the space between the entoglenoid process of the squamosal and the lateral edge of the anterior wall of the tympanic bulla. This space is marked by a deep incisure.

Tympanic region (Fig. 4). The tympanic bullae are very large, occupy a large part of the cranial base, and are closely positioned to each other (in the middle region, the distance between them is approximately 0.5 mm, while each bulla is more than 7 mm wide). The left bulla is well preserved.

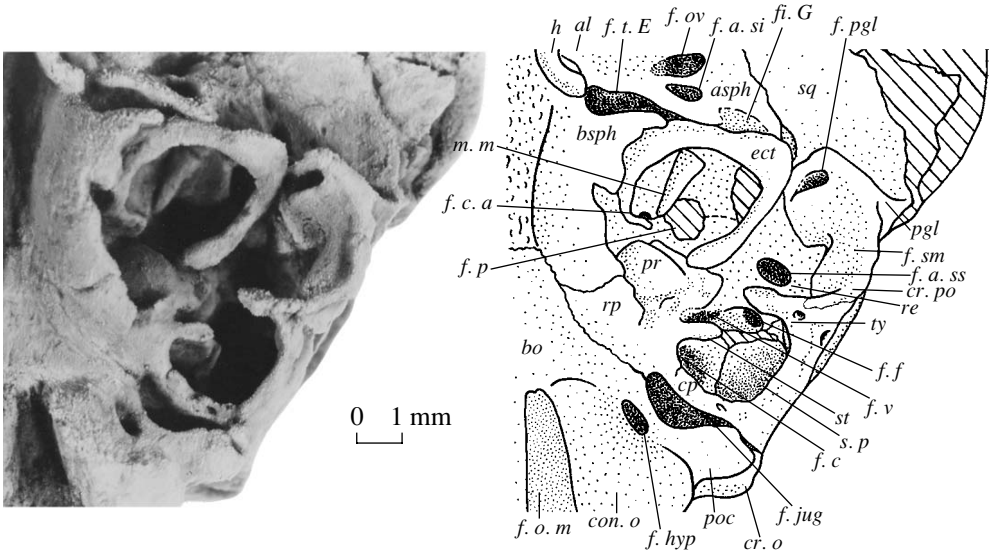

Fig. 4. *Scymnerix tartareus* sp. nov., holotype PIN, no. 3106/80, cranial base, left side. Designations: (*cp*) caudal tympanic process of the petrosal, (*cr. po*) crista parotica, (*f. a. si*) foramen for the ramus inferior of the stapedius artery, (*f. a. ss*) foramen for the ramus superior of the stapedius artery, (*f. c*) fossula for the cochlear fenestra, (*f. c. a*) anterior carotid foramen, (*f. f*) foramen facialis, (*f. ov*) foramen ovale, (*f. p*) rudimentary piriform fenestra and foramen for the major petrosal nerve, (*f. pgl*) postglenoid foramen, (*f. t. E*) foramen of the Eustachian tube, (*f. v*) vestibular fenestra, (*fi. G*) Glaserian fissure, (*h*) hamulus (hook of the alisphenoid process), (*m. m*) fragment of the manubrium of the malleus, (*pr*) promontory, (*re*) epitympanic recess, (*rp*) rostral tympanic process of the petrosal, (*s. p*) sinus of the petrosal, (*st*) stylohyal, and (*ty*) tympanohyal; for other designations, see Figs. 2 and 3.

Walls of the tympanic bulla are formed by the processes of the alisphenoid, basisphenoid, and petrosal and by the ectotympanic. The tympanic processes of the basisphenoid and alisphenoid are fused together to form the medial and anterior walls and the anteromedial region of the roof of the tympanic bulla. The anteromedial corner of the bulla is pierced by a very large foramen of the Eustachian tube, and the anterior wall is pierced by a foramen for the ramus inferior of the stapedius artery and a fissure between the lateral part of the ectotympanic and the tympanic process of the alisphenoid.

Near the boundary with the petrosal, the central part of the roof of the tympanic bulla contains a relatively large round foramen; this is probably a rudimentary piriform fenestra and a foramen of the major petrosal nerve. Medial to this foramen, near the anteromedial corner of the promontory, the petrosal–sphenoid suture contains a small anterior carotid foramen (for the promontory artery).

The rostral process of the petrosal reaches the suture between the basioccipital and basisphenoid and forms the posteromedial wall of the tympanic bulla. The caudal process of the petrosal limits the tympanic cavity posterolaterally and isolates the fossula for the cochlear fenestra (fen. cochleae s. rotunda) from the jugular foramen. Most of the roof of the tympanic bulla is formed by the petrosal. The projection of the petrosal (promontory) is large, strongly swollen, and occupies almost one-third of the tympanic cavity. Its anterior side has a well-pronounced sulcus for the promontory artery. The deep and wide sulcus for the proximal portion of the stapedius artery, which is located in the posterolateral corner of the promontory, forms an incisure in the ventral edge of the vestibular fenestra. A weak sulcus for the internal carotid artery extends medial to this point.

An extensive vestibular fenestra is located lateral to the promontory, and a large foramen facialis is anterolateral to this fenestra. The foramen for the ramus superior of the stapedius artery (for. spinosum sensu Butler, 1980) is a little anterior to the foramen facialis near the squamosal–petrosal suture. The squamosal does not participate in the formation of the roof of the tympanic bulla.

The ectotympanic is relatively small. It forms an incomplete ring (open on the posterior side for approximately one-third of its extent) for the attachment of the tympanic membrane (pars tensa membranae tympani). The tympanic ring is located anterior to the promontory and projects ventrally from under the tympanic processes of the basisphenoid and alisphenoid. The medial (ventral) portion of the tympanic ring is relatively narrow and only slightly curves (a sharp lateral curvature of its caudal end in the holotype is probably attributable to deformation). It contributes to the formation of the ventral wall of the auditory capsule. The lateral (dorsal or malleolar) portion is stout and sharply posteromedially curves. It separates the epitympanic recess from the portion of the tympanic cavity which is located rostral to the promontory. The rostral end of the lateral portion forms a relatively high petaloid crest, which curves somewhat anteriorly. This element of the ectotympanic

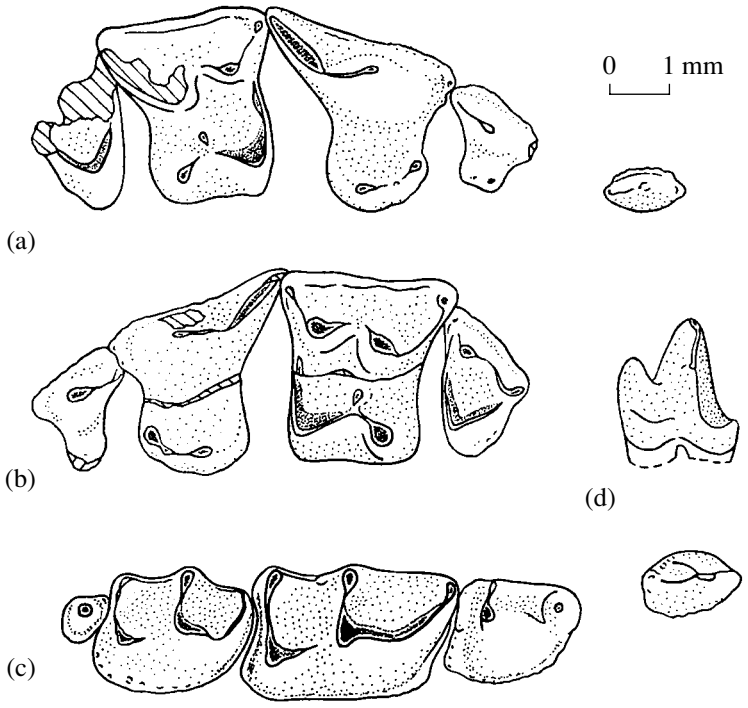

Fig. 5. *Scymnerix tartareus* sp. nov., holotype PIN, no. 3106/80, dentition: (a) right C^1 and P^3–M^2, (b) left P^3–M^2, (c) right C_1 and P_4–M_3, and (d) right P_4, lingual view.

is not fused with the tympanic process of the alisphenoid, they are separated from each other by a clear space. This is a relatively large transversely elongated fissure, which is open laterally; this area was most likely occupied by the Glaserian fissure, which provided passage for the chorda tympani. The caudal end of the lateral portion of the ectotympanic reaches the promontory, it is substantially thicker compared to the intermediate part of this portion. The medial portion of the tympanic ring is expanded. The angle between the oblique dorsoventral plane of the tympanic ring and the horizontal plane of the skull is approximately 25°.

A fragmentary small bone is preserved in the tympanic cavity; most likely, this is a fragment (rostral part) of the manubrium of the malleus (Fig. 4).

The epitympanic recess is deep and broad and formed by the mastoid. The suprameatal fossa located within the epitympanic wing of the squamosal is relatively deep, a little deeper than the glenoid fossa. The anterior and posterior edges of the suprameatal fossa are widely spaced. The ventral portion of the suture between the squamosal and the mastoid crosses the wall of the epitympanic recess along the tympanohyal. Anterior to the tympanohyal, the ventral wall of the suprameatal fossa forms a relatively large diverticulum, which is bordered laterally and posterolaterally by a clear crista parotica and provides an attachment area for the pars flaccida membranae tympani, which was also connected to the well-developed processes of the tympanohyal and stylohyal. The fossa for the stapedius muscle is deep (partially preserved on the left side). A large sinus of the petrosal is located dorsal to this fossa.

Upper dentition (Figs. 5a, 5b). Left P^3–M^2 and right C^1 and P^3–M^2 and the alveoli of left I^2, I^3, C^1, and P^2 and right P^2 are preserved in the skull. The alveoli of single-rooted I^2 and I^3 are small and oval in shape. I^2 is smaller than I^3. The alveolus of I^2 has a constriction, which suggests that the root was partially doubled. The diastema between I^3 and the canine is short. The canine is double-rooted, small, transversely compressed, and has a conical apex, small anterior and posterior cingular cuspules, and enamel sculpturing shaped into the longitudinal row of very small tubercles on the labial side. Judging from the alveolus, P^2 was single-rooted and smaller than the canine.

P^3 is three-rooted and slightly longer but much lower than the canine. The base of the paracone is located in the central area of the crown. The parastyle is weak, the metastyle is well developed and connected to the paracone by a well-pronounced metacrista. The internal lobe is well developed. The protocone is small and low. The labial side of the crown base has a longitudinal row of small tubercles.

P^4 is more than twice as large as P^3. The paracone is the most massive and high cusp, its height is at least four-fifth of the total crown length. The protocone is small and low and projects slightly anteriorly with reference to the paracone. The hypocone is located posterolingual to the protocone. It is more massive than the

latter but relatively low. Between the protocone and hypocone, there is a very small and low supplementary cuspule, which is connected to a short anterior crest of the hypocone. Posterior to the hypocone, the lingual region of the crown is flattened and expanded; a relatively sharp cingulum is observed in the posterolingual corner. The parastyle is small and weak. The long metacrista is connected to a poorly developed metastyle. The carnassial notch between the metacrista and the posterior base of the paracone is well developed. The narrow and continuous labial cingulum extends from the parastyle to the level of the metastyle. In its structure, one can recognize widely spaced small tubercles, which are especially well-pronounced in the anterior region of the cingulum. The tooth has three stout roots.

M^1 is the largest tooth in the row, it is a little wider and slightly shorter than P^4. The paracone is the highest main cusp of M^1, it is substantially lower than the paracone of P^4. The paracone is located anterolabial to the metacone and connected to the latter by a low centrocrista. The metacone is only slightly lower than the paracone. The third highest cusp of the tooth, the protocone, is located more lingually than the paracone and is slightly displaced anteriorly with reference to the apex of the latter. The hypocone is located posterolingual to the protocone, and its apex is slightly displaced posteriorly in relation to the apex of the metacone. The anterolabial corner of the protocone is connected to the anterolingual side of the paracone base by a well-developed preprotocrista and a small preparaconule crest. The paraconule is undeveloped. The postprotocrista is posterolabially directed. At the tooth center, it bifurcates; the first arm turns posterolingually and adjoins the hypocone, while the second arm retains the initial direction and is connected to a small and low conical metaconule. The parastyle is small, the paracrista is weak and shaped into a poorly pronounced anterolingual ridge of the paracone. The metastyle is relatively large; the metacrista is stout, at least one-fourth as long as the total labial length of the crown. The labial cingulum is well developed, continuous, and narrow. The bases of the labial and lingual sides of the crown are covered by weak sculpturing of small enamel tubercles. The labial roots are widely spaced, while the lingual root is integral.

M^2 is small and lacks a hypocone. The relatively high paracone and low reduced metacone are widely spaced. The metacone is strongly lingually displaced with reference to the paracone. The centrocrista is low. The protocone is massive, the preprotocrista terminates on the lingual side of the paracone base, the postprotocrista terminates on the lingual side of the metacone base, and the metaconule is absent. The parastyle is relatively large and well developed, while the metastyle is absent. The labial cingulum extends from the parastyle to the level of the anterior base of the metacone. The base of the posterolingual side of the crown is covered by weak sculpturing composed of enamel tubercles. The tooth is three-rooted, the posterior labial root is substantially reduced and projects beyond the edge of the palatal process of the maxilla.

Lower jaw (Fig. 3b). The horizontal ramus of the lower jaw is narrow and low. The angle between the right and left mandibular rami is small, approximately 20°. The symphysis extends posteriorly to P_3. The mental foramen is small and located in line with the middle of P_4 near the ventral edge of the horizontal ramus. Under the molars, there is an extensive depression, which was probably the attachment area for the anteriorly displaced portion of the masticatory muscle (m. masseter).

The ascending ramus of the lower jaw is relatively long and substantially labially curved with reference to the middle line of the jaw. The angle between the anterior edge of the base of the ascending process and the horizontal ramus is approximately 100°. In the dorsal part, the ascending process gently curves posteriorly; its apex is hooked. The base of the coronoid process is separated from the posterior edge of M_3 by a small space. The medial ridge at the base of the coronoid process, which provided the attachment area for a portion of the temporal muscle, is wide and stout. The masseteric fossa is relatively superficial. The mandibular foramen is large and located in the middle of the ascending ramus on level with the alveolar edge of the jaw. The articular process is short. The condyle is wide and located on level with the tooth row, its posterior surface is flattened. The incisure between the articular and angular processes is deep. The angular process is large, lobate, and strongly curved medially. Its medial side has a stout horizontal ridge bordering a depression for the attachment of the internal pterygoid muscle.

Lower dentition (Figs. 5c, 5d). In the lower jaw, both I_2, left and right P_4–M_3, and right C_1 are preserved. The anterior incisor is stout and straight; its crown is semicircular in section, i.e., the medial side is straight. The labial side of the crown base is covered by very small and randomly scattered tubercles. I_3–P_3 are single-rooted. The alveoli of I_3 are represented by only the medial walls; judging from these alveoli, I_3 was a small tooth positioned close to I_2. The canine is small, the anterior part of its crown is raised in a characteristic manner. Two crests descend from the low main cusp to a small posterior cuspule; the central crest is sharp and long, and the lingual crest is shorter and poorly developed. The base of the labial side of the crown is ornamented by a longitudinal row of small enamel tubercles. Judging from the alveolus, P_3 is at most as large as the canine.

P_4–M_2 are exoedaenodont (the labial edge of these teeth strongly projects beyond the jaw edge, while the cusps are lingually inclined), high, and narrow at the apex; however, their bases expand labially. P_4 is relatively short and has a high and well-differentiated trigonid and a reduced talonid. The well-developed paraconid is separated from the protoconid by a deep notch.

The protoconid is conical and pyramidal, and its lingual base is fused with the rudimentary metaconid. The apices of the protoconid and metaconid are connected to each other by the short and straight crest of the protocristid. The posterior edge of the talonid is bordered by a well-pronounced postcingulid. The labial surface of the crown has a sharp and narrow precingulid and three longitudinal rows of enamel tubercles: the upper row extends from the precingulid to the posterolabial side of the talonid, the middle row is located somewhat lower and follows along the upper row, and the lower row includes five or six tubercles at the base of the posterolabial corner of the crown.

M_1 is large and elongated. The talonid is approximately half as long as the trigonid; however, it is of almost the same width. The paraconid strongly projects anteriorly, the paralophid is stout and curves slightly labially. The metaconid is relatively massive, low, located in the same transverse line as the protoconid, and fused with the latter at the base. The apices of the metaconid and protoconid are isolated from each other by a weak notch. The talonid basin is closed by the longitudinally extended entoconid with a well-developed entocristid and a small and distinct metastylid. The talonid notch is present. The hypoconid slightly projects posteroexternally. The cristid oblique adjoins the middle of the posterior wall of the protoconid. The narrow postcingulid extends from the posterolabial side of the hypoconid to the middle of the posterior wall of the crown. The precingulid is stout and borders the anterolabial side of the crown base on level with the anterior region of the paralophid. The labial side has two longitudinal rows of enamel tubercles; the upper row extends from the precingulid to the postcingulid, and the lower row extends from the anterolabial corner to the posterolabial corner of the crown base (it is broken on level with the apex of the protoconid). The surface of the labial walls of the protoconid and hypoconid is uneven because of the rough enamel.

M_2 is almost 1.5 times shorter than M_1. The trigonid and talonid are approximately equal in length and width. M_2 is similar in structure to M_1; however, it differs in the shorter paralophid, a more strongly posteriorly projecting hypoconid, relatively small entoconid, and a weak entocristid. The precingulid and postcingulid are weak. The labial surface has a row of relatively large enamel tubercles extending from the precingulid to the postcingulid.

M_3 is rudimentary, single-rooted, and columnlike. It is one-fifth as long as M_1 and less than one-third as long as M_2. The crown is oval in plan and has a conical protoconid, a low and anteriorly projecting paraconid, and a well-pronounced labial cingulid, which is posterolabially convex.

Occlusion. In the occludent state (before preparation), the apex of the upper canine is opposed by that of the lower canine; the paraconid of P_4 is opposed by the parastyle of P^3, and the blade of the anterior side of the protoconid of P_4 is opposed by the blade of the posterior side of the paracone of P^3. The main cutting function was performed by the blades of the metacrista of P^4 and the paralophid of M_1. In the occludent state, they are opposed to each other; the paracone of P^4 is located lingual to the paraconid of M_1; the talonid of M_1 is opposed by the anterior region of M^2, the trigonid of M_2 is opposed by the posterior region of M^1, the talonid of M_2 is opposed by the paracone and protocone of M^2, and M_3 is opposed by the metacone of M^2 (Fig. 1).

Measurements, mm. Greatest skull length (rostrum is partially broken off), ca. 30; zygomatic width (right zygomatic arch is reconstructed), ca. 21; frontal width at the interorbital constriction, 6.5; greatest width of the braincase region of the skull (without regard for deformation), ca. 15; length from the interorbital constriction to the posterior skull edge, 17.0; (A) distance from the anterior edge of the maxilla to the transverse palatal crest, 13.0; (B) width of the palate at P^2, 6.5; index of palatal extension (A/B, see Rich and Rasmussen, 1973, table 5), 2.0; and palatal width between the lingual edges of M^1, 6.0.

Length of the upper tooth rows, (sin.) left and (dex.) right sides: I^2–M^2, 13.7 (sin.); C^1–M^2, 10.4 (dex.); P^3–M^2, 8.5 (sin.) and 8.4 (dex.); P^4–M^2, 7.1 (sin.) and 7.2 (dex.); and M^1–M^2, 4.1 (sin.) and 4.2 (dex.). Alveoli (length × width): I^2 (sin.), 1.0×0.75; I^3 (sin.), 1.1×0.8; P^2, 0.8×0.5 (sin.) and 0.9×0.5 (dex.). Upper teeth (length × width × maximal labial height): C^1 (dex.), $1.35 \times 0.75 \times 1.4$; P^3, $1.75 \times 1.5 \times 1.2$ (sin.) and $1.75 \times 1.4 \times 1.2$ (dex.); P^4, $3.35 \times 2.85 \times 3.25$ (sin.) and $3.3 \times 2.85 \times 3.0$ (dex.); M^1, $3.0 \times 3.3 \times 1.5$ (sin.) and $2.9 \times 3.3 \times 1.5$ (dex.); and M^2, $1.65 \times 2.55 \times 0.7$ (sin.) and $1.75 \times 2.55 \times 0.7$ (dex.).

Lower jaw: total length of the jaw along the midline, 25.8; length of the right mandibular ramus from I_2 to the articular condyle, 23.0; length from the articular ridge to the posterior edge of M_3, 8.3; depth of the lower jaw at the coronoid process, 9.2; under P_4, 2.9; posterior to M_3, 3.2; thickness of the horizontal ramus posterior to M_3, 1.7. Length of the lower tooth row from the anterior base of I_2 to the posterior edge of M_3, 14.7 (sin.) and 14.8 (dex.). Lower teeth (length × width × labial height): C_1, $1.6 \times 1.1 \times 1.2$ (dex.); P_4, $2.5 \times 1.8 \times 3.2$ (sin., dex.); M_1, $3.8 \times 2.4 \times 3.0$ (sin., dex.); M_2, $2.6 \times 1.9 \times 2.2$ (sin., dex.); M_3, $0.8 \times 0.65 \times 0.8$ (sin.) and $0.7 \times 0.7 \times 0.8$ (dex.).

Remarks. In living insectivores, skull length is closely associated with body weight (Thewissen and Gingerich, 1989). The logarithmic relationship is described by the formula $Y = 3.68X - 3.83$ (where X is the logarithm of the skull length, mm; and Y is the logarithm of the body weight, g). The total skull length of *Scymnerix tartareus* is approximately 31 mm; this allows one to estimate its weight as being approximately 45–50 g and, thus, to assign it to the weight

group of extant shrew-hedgehogs of the genus *Hylomys* (Strel'nikov, 1970; Gureev, 1979).

M a t e r i a l. Holotype.

DISCUSSION

The cranial structure of *Scymnerix tartareus* strongly suggests that it belongs to the subfamily Erinaceinae. However, the skull and dental system of *Scymnerix* display a number of interesting features, which deserve special consideration.

The short facial region of the skull, the structure of the zygomatic arch, large I_2, single-rooted I^3, small C^1, reduced M^2, the absence of M^3, and the presence of the enamel sculpturing on the teeth show that *S. tartareus* is similar to short-faced hedgehogs of the subfamily Brachyericinae. However, the auditory region of *Scymnerix* lacks distinctive structural characteristics of the Brachyericinae (see Rich and Rich, 1971; Rich, 1981; Gould, 1995). In particular, its tympanic bullae are not closed ventrally and ossified intratympanic arterial canals are absent. On the contrary, the structure of the auditory region gives clear evidence for the assignment of *Scymnerix* to the Erinaceinae. In addition, *Scymnerix* differs from the Brachyericinae in the position of the lacrimal foramen, the presence of the palatine fissures, a very large interparietal, the absence of a sagittal crest, poorly developed paroccipital processes, the presence of P^2, the better developed protocone of P^3, the presence of the metaconule on M^1, the absence of a well-pronounced and long masseter ridge on the lower jaw, relatively large P_4 with a clearly differentiated trigonid, the shape of the trigonid of M_1 and M_2, and the preservation of rudimentary M_3. Apparently, the similarity of *Scymnerix* and brachyericines in the structure of the facial region of the skull and the reduction of intermediate antemolars and posterior molars is a result of parallel development associated with the shortening of the snout.

The shortening of the facial region in *Scymnerix* has a direct bearing on the arrangement of the upper cheek teeth and structures of the orbital region: the infraorbital foramen is located above the central region of P^3, the anterior orbital rim is above the anterior region of P^4, and the base of the zygomatic arch is on level with M^1. This structural pattern is characteristic of the Brachyericinae (Matthew and Mook, 1933; Rich and Rich, 1971; Rich, 1981; Qiu and Gu, 1988), while in other Erinaceidae, the infraorbital foramen is usually located above P^4 or P^3/P^4, the anterior orbital rim is above M^1, and the base of the zygomatic arch is above M^1/M^2. Among the Erinaceinae, an exception is provided by some Miocene Amphechinini, in particular, European *Dimylechinus bernoullii*, which is characterized by the loss of M^3 and M_3 (Hürzeler, 1944), and African *Amphechinus rusingensis* (Butler, 1956).

The reduction of the tooth row of *Scymnerix* manifests itself in a decrease in the number of roots in I^3 and P^2; a decrease in the size of C^1; and reduction of M^2, M_2, and M_3. M^2 is more strongly reduced than that of *Dimylechinus* (Hürzeler, 1944), since it has lost the hypocone. M_3 is reduced to a much greater extent than that of Amphechinini and Erinaceini. In erinaceids that have lost M^3, M_3 is usually absent as well (Brachyericinae, *Dimylechinus*); otherwise, both teeth are partially reduced, as is observed in the majority of Amphechinini and all Erinaceini. *Scymnerix* is an exception in this respect as well. The Lipotyphla provide certain other examples of the presence of strongly reduced M_3 combined with the absence of M^3, e.g., *Exoedaenodus* (Dimylidae) and *Suleimania* (Talpidae) (Ziegler, 1990; Hoek-Ostende, 2001). The increased anterior incisors are characteristic not only of the Brachyericinae but also of Amphechinini.

The presence of the antorbital fossa is a distinctive character of small Galericinae, Brachyericinae, and Amphechinini; this is probably associated with their small size (Butler, 1948). The position of the lacrimal foramen on the antorbital crest (in contrast to its position inside the orbit) is a derived character typical of the tribe Erinaceini. The lacrimal duct is seen from the lateral side in Protericini, Brachyericinae, and Erinaceinae. In Protericini, Brachyericinae, and Amphechinini, the lacrimal foramen opens in the orbit, while in Erinaceini and *Scymnerix*, it opens in the antorbital crest. Within the subfamily Erinaceinae, the small palatine fissures and the absence of a nasopharyngeal fossa is only characteristic of the tribe Amphechinini. The large interparietal is a primitive character typical of the Galericinae and some Amphechinini (Butler, 1948, 1956). In Erinaceini, Brachyericinae, and Protericini, the anterior edge of the occipital condyles is nonemarginated. The postglenoid foramen isolated from the glenoid fossa by the entoglenoid process is a primitive character, which distinguishes *Scymnerix* and Amphechinini from Erinaceini. The weak paroccipital processes and a low position of the mandibular condyle (on level with the tooth row) are also characteristic of Amphechinini.

The ectotympanic (tympanic ring) of *Scymnerix* resembles that of the Galericinae and *Amphechinus* in size and shape (Viret, 1938; Butler, 1948). The tympanic bone and ear ossicles are scarce in the fossil record. Therefore, notwithstanding the availability of extensive material on the auditory region of extinct Erinaceidae (Viret, 1938; Butler, 1948, 1956, 1980; Gawn, 1968; Rich and Rich, 1971; Rich, 1981; MacPhee *et al.*, 1988; Gould, 1995; Meng *et al.*, 1999), the data on the structure of the ectotympanic are rather scarce. *Scymnerix* displays the semiphanery, i.e., partial fusion of the ectotympanic with other components of the floor of the tympanic bulla, which is typical of erinaceids; the Brachyericinae are characterized by the aphanery, i.e., their ectotympanic is completely covered by the auditory capsule, which is formed by the sphenoid and petrosal (MacPhee *et al.*, 1988).

Thus, the cranial structure suggests that *Scymnerix* belongs to the subfamily Erinaceinae. A number of structural features of the skull and dentition clearly distinguish *Scymnerix* from Amphechinini and Erinaceini; thus, this genus should be assigned to a new tribe, Scymnericini.

The shortening of the snout in the Brachyericinae is associated with the carnivorous specialization (Lopatin, 1996, 1999; Lopatin and Zazhigin, 2003) or adaptation to feeding on prey provided with the firm cover (McKenna and Holton, 1967) or "mechanically rough food," including plants (Gureev, 1979, pp. 76, 140). The rugosity of the dental enamel is commonly regarded as an indicator of adaptation to a high load. The structure of teeth and lower jaw of *Scymnerix* lacks the characters of carnivorous adaptation, which are typical of the Brachyericinae (see Lopatin and Zazhigin, 2003). Structural dental features of this hedgehog can be interpreted as a result of adaptation to feeding on firm vegetative and animal food.

ACKNOWLEDGMENTS

I am grateful to A.K. Agadjanian (PIN) for useful discussion of the material.

The study was supported by the Russian Foundation for Basic Research, project nos. 00-15-97754, 01-05-65448, 02-04-48458, and 02-04-06299, and the American Paleontological Society (PalSIRP Sepkoski Grants).

REFERENCES

Butler, P.M., On the Evolution of the Skull and Teeth in the Erinaceidae, with Special Reference to Fossil Material in the British Museum, *Proc. Zool. Soc. London, Ser. B*, 1948, vol. 118, pp. 446–500.

Butler, P.M., Erinaceidae from the Miocene of East Africa, *Brit. Mus. Natur. Hist. Fossil Mammals Africa*, 1956, vol. 11, pp. 1–75.

Butler, P.M., The Giant Erinaceid Insectivore, *Deinogalerix* Freudenthal, from the Upper Miocene of Gargano, Italy, *Scripta Geol.*, 1980, no. 57, pp. 1–72.

Frost, R., Wozencraft, W.Ch., and Hoffmann, R.S., Phylogenetic Relationships of Hedgehogs and Gymnures (Mammalia: Insectivora: Erinaceidae), *Smithson. Contrib. Zool.*, 1991, no. 518, pp. 1–50.

Gawn, C.E., The Genus *Proterix* (Insectivora, Erinaceidae) of the Upper Oligocene of North America, *Am. Mus. Novit.*, 1968, no. 2315, pp. 1–26.

Gould, G.C., Hedgehog Phylogeny (Mammalia, Erinaceidae)—The Reciprocal Illumination of the Quick and the Dead, *Am. Mus. Novit.*, 1995, no. 3131, pp. 1–45.

Gureev, A.A., Insectivores (Mammalia, Insectivora): Hedgehogs, Moles, and Shrews (Erinaceidae, Talpidae, Soricidae), *Fauna SSSR. Mlekopitayushchie* (Fauna of the USSR: Mammals), Leningrad: Nauka, 1979, vol. 4, no. 2.

Hoek Ostende, L.W., van den., Insectivore Faunas from the Lower Miocene of Anatolia: 5. Talpidae, *Scripta Geol.*, 2001, no. 122, pp. 1–45.

Huang, X., Fossil Erinaceidae (Insectivora, Mammalia) from the Middle Oligocene of Ulantatal, Alxa Zouqi, Nei Mongol, *Vertebr. Palasiat.*, 1984, vol. 22, no. 4, pp. 305–309.

Hürzeler, J., Über einem dimyloiden Erinaceiden (*Dimylechinus* gen. nov.) aus dem Aquitanien der Limagne, *Eclog. Géol. Helv.*, 1944, vol. 37, no. 2, pp. 460–467.

Klaauw, C.J., van der., The Auditory Bulla in Some Fossil Mammals, with a General Introduction to This Region of the Skull, *Bull. Am. Mus. Natur. Hist.*, 1931, vol. 62, art. 1, pp. 1–352.

Lopatin, A.V., Stratigraphy and Small Mammals from the Aral Formation of the Altynshokysu Locality (Northern Aral Region), *Stratigr. Geol. Korrelyatsiya* (Moscow), 1996, vol. 4, no. 2, pp. 65–79.

Lopatin, A.V., Oligocene and Early Miocene Insectivores (Insectivora, Mammalia) from Western Kazakhstan, *Paleontol. Zh.*, 1999, no. 2, pp. 66–75.

Lopatin, A.V., The Largest Asian *Amphechinus* (Erinaceidae, Insectivora, Mammalia) from the Oligocene of Mongolia, *Paleontol. Zh.*, 2002, no. 3, pp. 75–80.

Lopatin, A.V. and Zazhigin, V.S., New Brachyericinae (Erinaceidae, Insectivora, Mammalia) from the Oligocene and Miocene of Asia, *Paleontol. Zh.*, 2003, no. 1, pp. 64–77.

MacPhee, R.D.E., Novacek, M.J., and Storch, G., Basicranial Morphology of Early Tertiary Erinaceomorphs and the Origin of Primates, *Am. Mus. Novit.*, 1988, no. 2921, pp. 1–42.

Matthew, W.D. and Granger, W., New Insectivores and Ruminants from the Tertiary of Mongolia, with Remarks on the Correlation, *Am. Mus. Novit.*, 1924, no. 105, pp. 1–7.

Matthew, W.G. and Mook, C.C., New Fossil Mammals from the Deep River Beds of Montana, *Am. Mus. Novit.*, 1933, no. 601, pp. 1–7.

McDowell, S.B., The Greater Antillean Insectivores, *Bull. Am. Mus. Natur. Hist.*, 1958, vol. 115, art. 3, pp. 113–214.

McKenna, M.C. and Holton, C.P., A New Insectivore from the Oligocene of Mongolia and a New Subfamily of Hedgehogs, *Am. Mus. Novit.*, 1967, no. 2311, pp. 1–11.

Mellett, J.S., The Oligocene Hsanda Gol Formation, Mongolia: A Revised Faunal List, *Am. Mus. Novit.*, 1968, no. 2318, pp. 1–16.

Meng, J., Ye, J., Wu, W.-Y., and Bi, Sh.-D., The Petrosal Morphology of a Late Oligocene Erinaceid from North Junggar Basin, *Vertebr. Palasiat.*, 1999, vol. 37, no. 4, pp. 300–308.

Novacek, M.J., The Skull of Leptictid Insectivorans and the Higher-Level Classification of Eutherian Mammals, *Bull. Am. Mus. Natur. Hist.*, 1986, vol. 183, art. 1, pp. 1–112.

Qiu, Z.X. and Gu, Z.G., A New Locality Yielding Mid-Tertiary Mammals near Lanzhou, Gansu, *Vertebr. Palasiat*, 1988, vol. 26, no. 3, pp. 198–213.

Rich, T.H.V., Origin and History of the Erinaceinae and Brachyericinae (Mammalia, Insectivora) in North America, *Bull. Am. Mus. Natur. Hist.*, 1981, vol. 171, pp. 1–116.

Rich, T.H.V. and Rasmussen, D.L., New North American Erinaceine Hedgehogs (Mammalia: Insectivora), *Occas. Pap. Mus. Natur. Hist. Univ. Kansas*, 1973, no. 21, pp. 1–54.

Rich, T.H.V. and Rich, P.V., *Brachyerix*, a Miocene Hedgehog from Western North America, with a Description of the Tympanic Region of *Paraechinus* and *Podogymnura*, *Am. Mus. Novit.*, 1971, no. 2477, pp. 1–59.

Storch, G. and Dashzeveg, D., *Zaraalestes russelli*, a New Tupaiodontine Erinaceid (Mammalia, Lipotyphla) from the Middle Eocene of Mongolia, *Geobios*, 1997, vol. 30, no. 3, pp. 437–445.

Strel'nikov, I.D., *Anatomo-fiziologicheskie osnovy vidoobrazovaniya pozvonochnykh* (Anatomical and Physiological Foundation of Speciation in Vertebrates), Leningrad: Nauka, 1970.

Sulimski, A., On Some Oligocene Insectivore Remains from Mongolia, *Palaeontol. Pol.*, 1970, no. 21, pp. 53–70.

Thewissen, J.G.M. and Gingerich, P.D., Skull and Endocranial Cast of *Eoryctes melanus*, a New Palaeoryctid (Mammalia: Insectivora) from the Early Eocene of Western North America, *J. Vertebr. Paleontol.*, 1989, vol. 9, no. 4, pp. 459–470.

Trofimov, B.A., Insectivores of the Genus *Palaeoscaptor* from the Oligocene of Asia, *Tr. Paleontol. Inst. Akad. Nauk SSSR* (Moscow), 1960, vol. 77, no. 4, pp. 35–40.

Viret, J., Étude sur quelques Erinaceidés fossiles spécialement sur le genre *Palaerinaceus*, *Mém. Trav. Lab. Geol. Univ. Lyon*, 1938, vol. 34, no. 28, pp. 1–32.

Ziegler, R., Didelphidae, Erinaceidae, Metacodontidae und Dimylidae (Mammalia) aus dem Oberoligozän und Untermiozän Süddeutschlands, *Stuttgart. Beitr. Naturk., Ser. B*, 1990, no. 158, pp. 1–99.